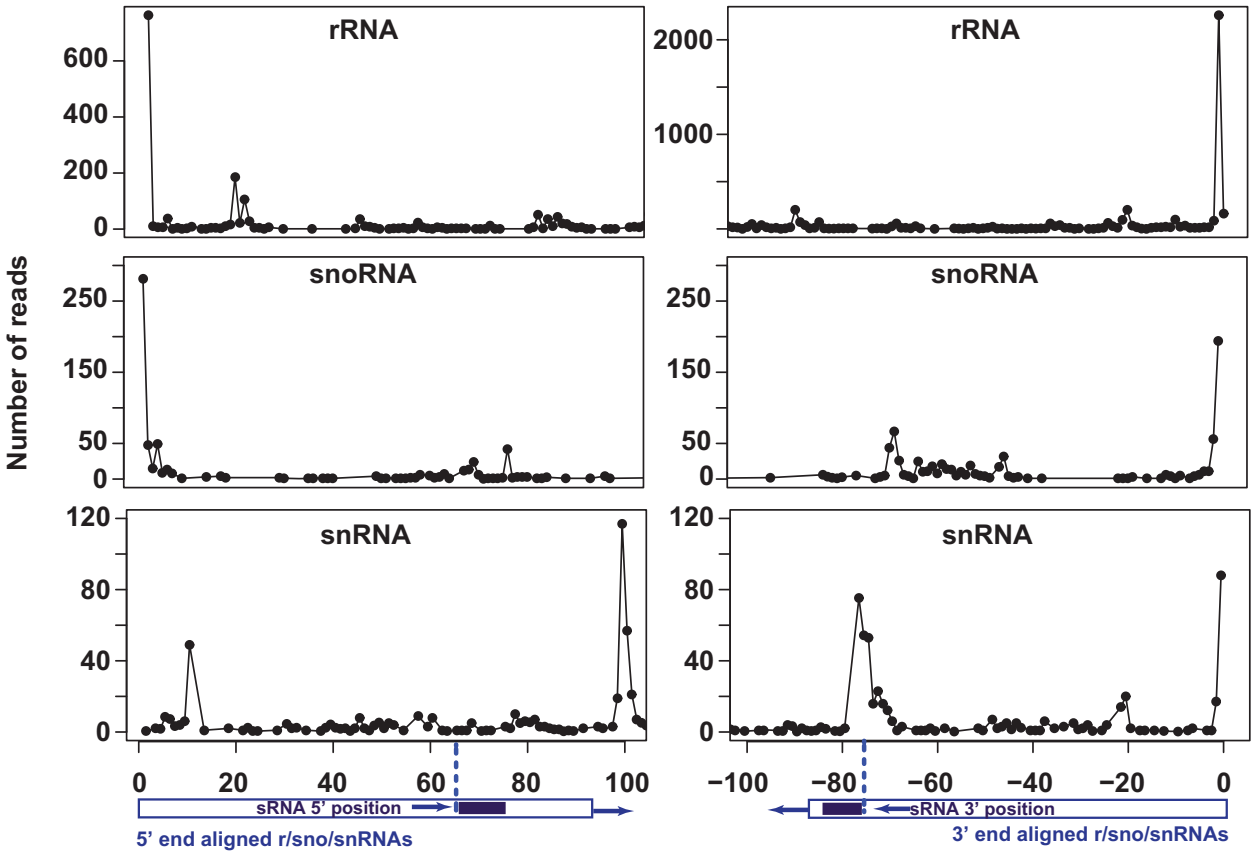

Figure S1. Comparison of abundance of RNA fragments deriving from rRNAs and snoRNAs, and snRNA in BCP1. Analysis indicate that the 3' and 5' terminal small RNAs are cloned multiple times, and that rRNA-derived reads are more abundant than snoRNAs and snRNAs, but less abundant than tRFs.

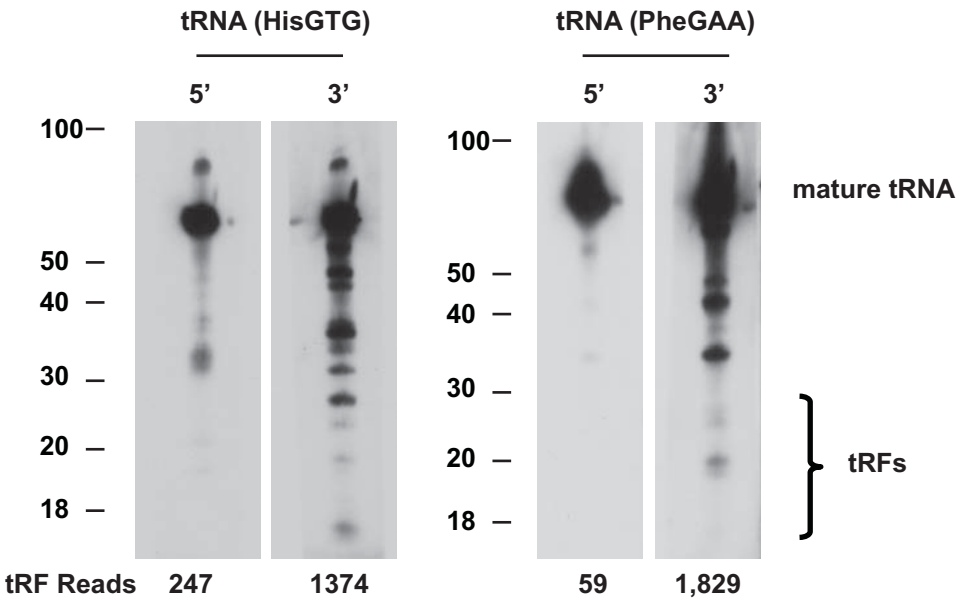

Figure S2. Comparison of abundance of 5' and 3' tRFs of two distinct tRNAs (HEK 293). Consistent with the deep sequencing results (tRF reads), the 3' tRF intensities are considerably more than that of the 5' tRFs in both cases.

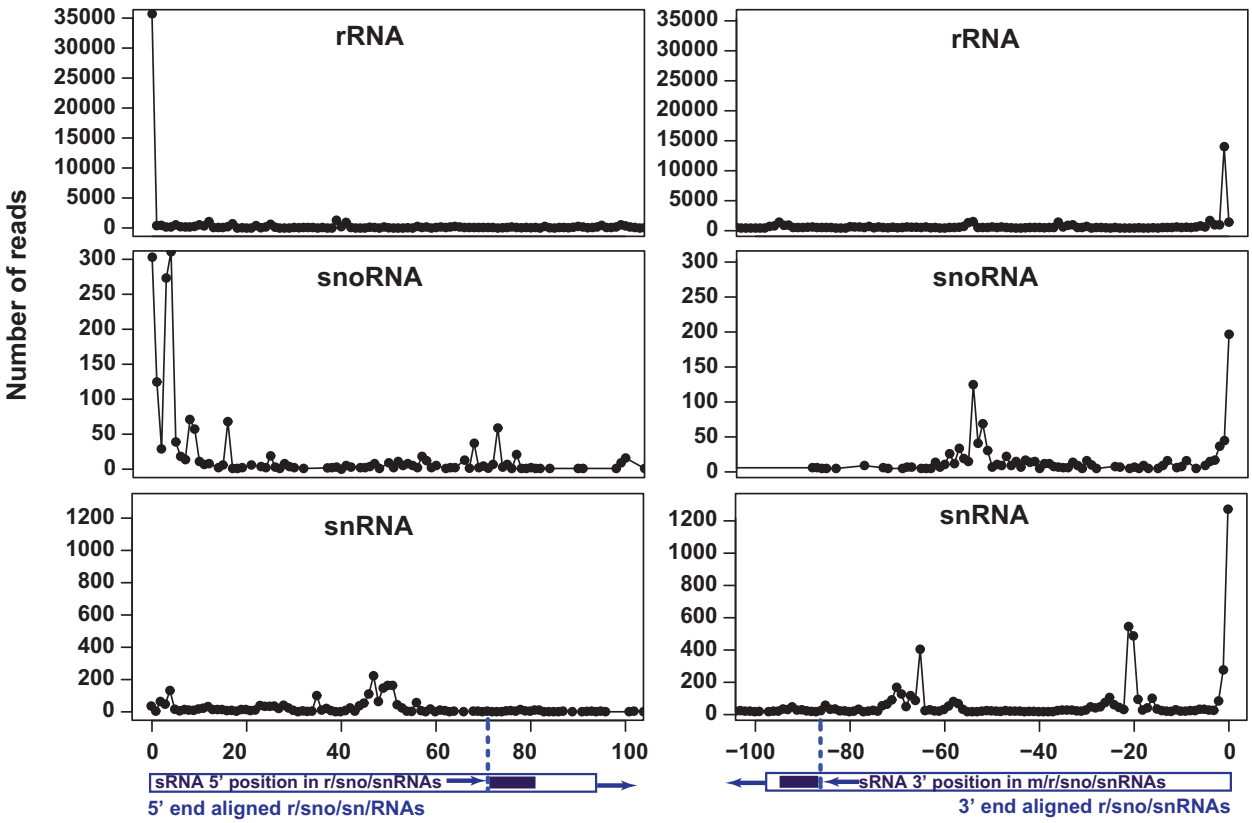

Figure S3. Small terminal 5'/3' RNA fragments of rRNAs and snoRNAs, 3' snRNA are present in mouse embryonic stem cells. Similar to human terminal RNA fragments, rRNA-derived fragments are more abundant than snoRNAs, and snRNAs, but less than that of mouse tRFs (**Figure 4A**).

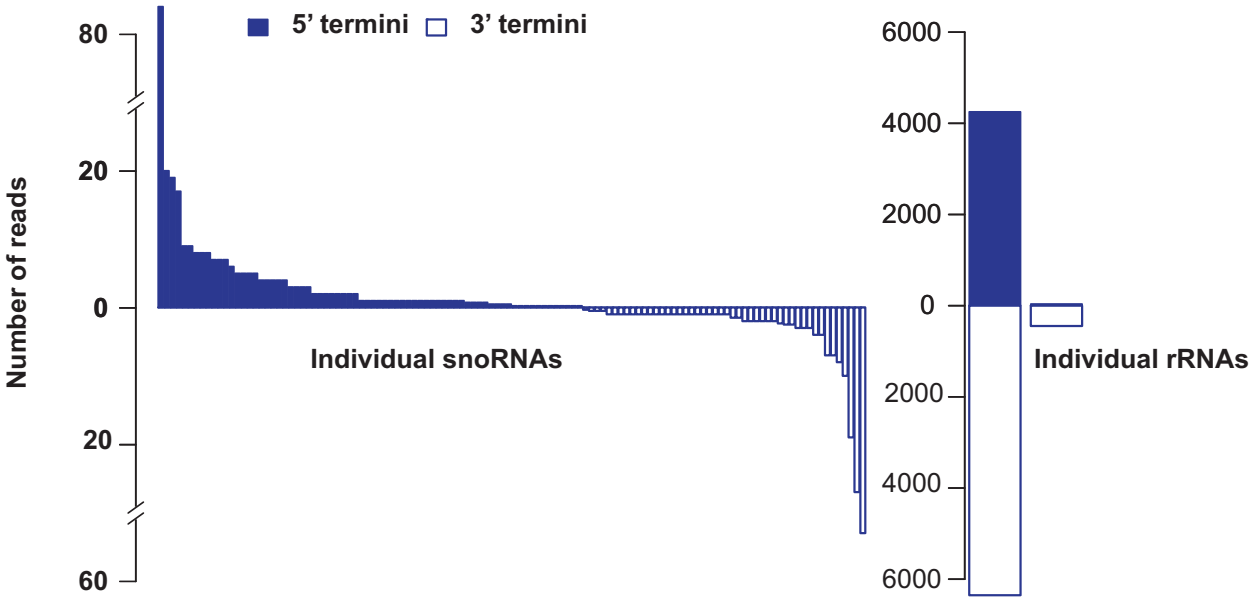

Figure S4. Strand bias of snoRNAs (left) and rRNAs (right) in mouse embryonic stem cells. X axis represents one individual snoRNA or rRNA.

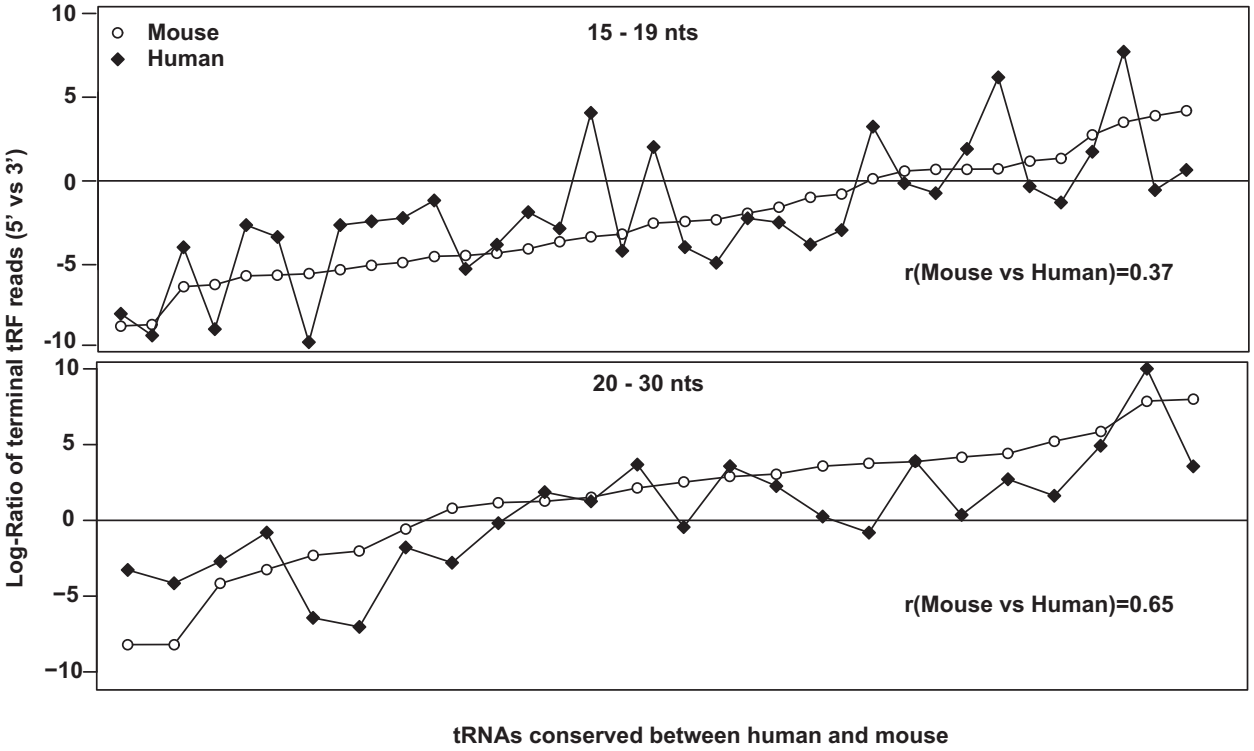

Figure S5. Comparison between asymmetric processing of human and mouse putative tRNA orthologs. Sequencing data of tRFs (reads/million ≥ 10) human 293 cells and mES cells are used for comparison.

A

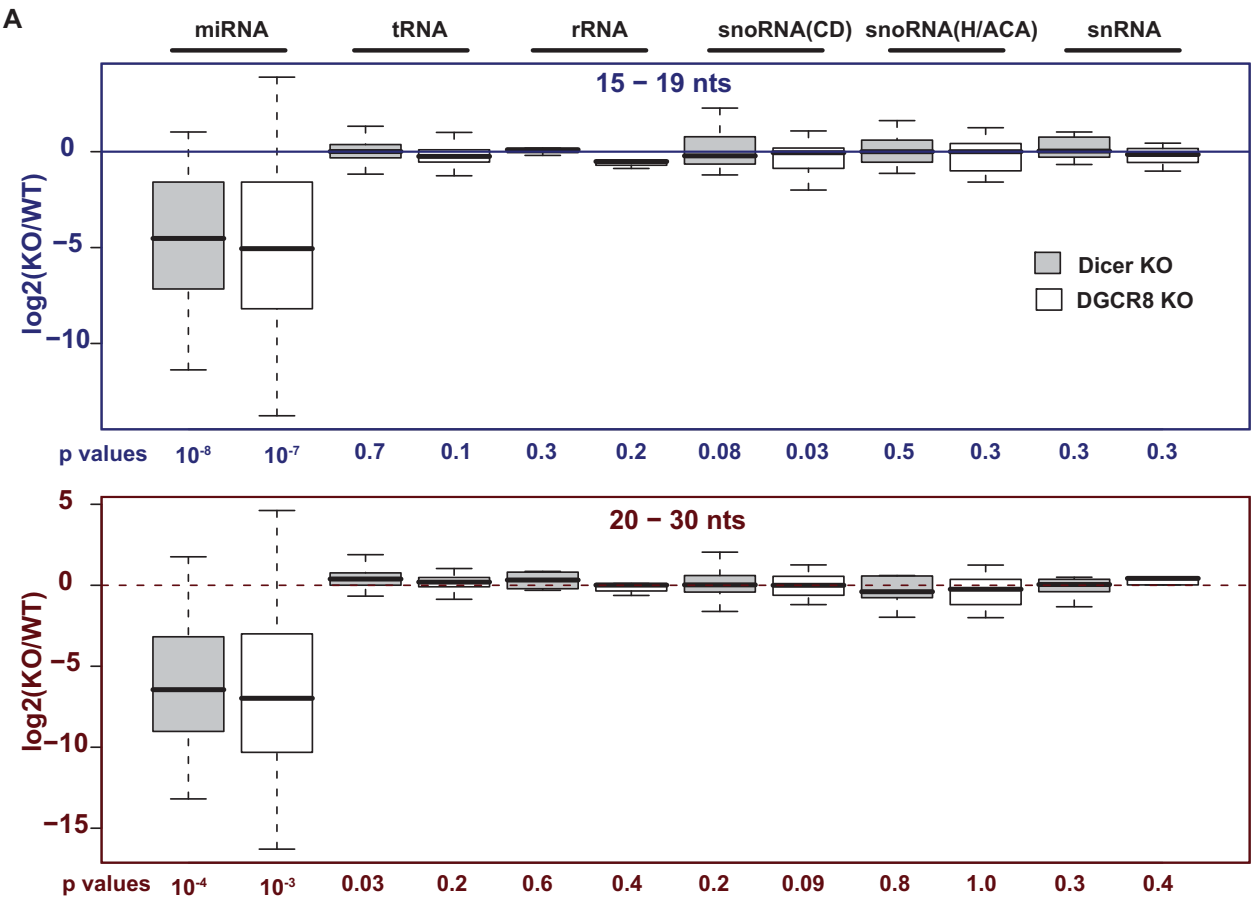

B

		15 − 19 nts			20 − 30 nts		
		WT	DicerKO	DGCR8KO	WT	DicerKO	DGCR8KO
tRNA	chr10.trna1282-TrpCCA	75	37	31	3	3	3
	chr13.trna101-TyrGTA	549	59	136	42	41	32
	chr2.trna1431-HisGTG	263	21	90	28	24	26
	chr3.trna28-TyrGTA	586	57	149	41	28	34
snoRNA	SNORA41 (H/ACA box)	8	4	3	0	0	0
	SNORA72 (H/ACA box)	3	2	2	7	2	2
	SNORD20 (CD box)	83	36	58	155	65	74
snRNA	U11	1	2	2	8	3	4
	U4	602	493	298	1221	265	235

Figure S6. Terminal small RNAs are largely independent of Dicer and Dgcr8 processing. (**A**) Boxplots based on log2-ratio (WT vs KO) of the RNA reads. Median (bar) and standard interquartile range (IQR) outliers (whiskers, 1.5x IQR) are represented along with p-values (paired t-tests). Small RNA classes other than miRNAs do not manifest an overall dependence on Dicer/DGCR8. (**B**) List of terminal RNAs that are down-regulated (>2 fold) upon both Dicer and Drosha KOs at either the 15–19 or 20–30 base long RNA groups.

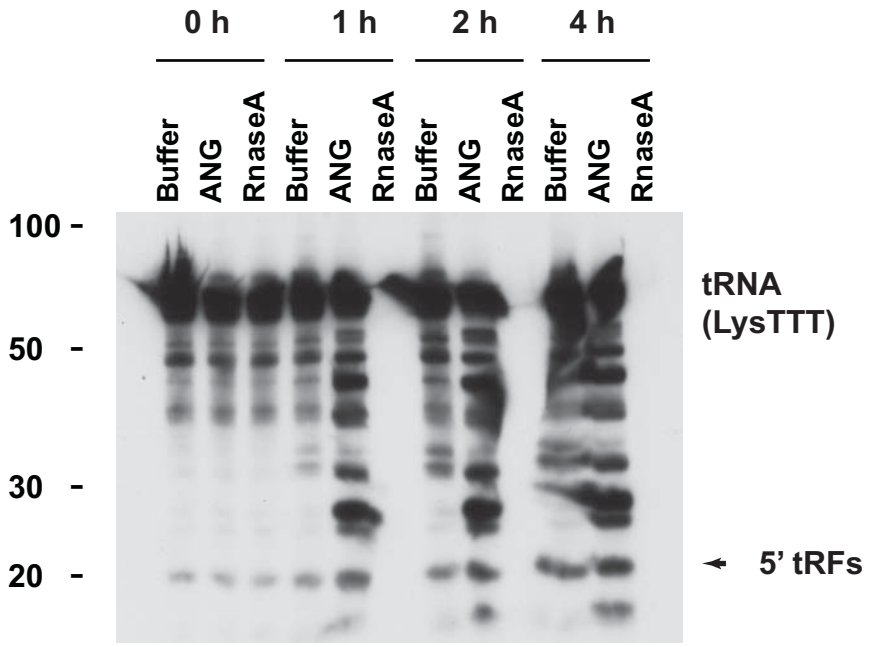

Figure S7. ANG can generate 5' tRFs. Total RNA from 293 cells were subject to cleavage by control buffer, RNase A (10 μg/ml), and ANG (10 μg/ml). ANG enhances the expression of the endogenous small fragment (~ 20 nts) in a time-dependent manner.

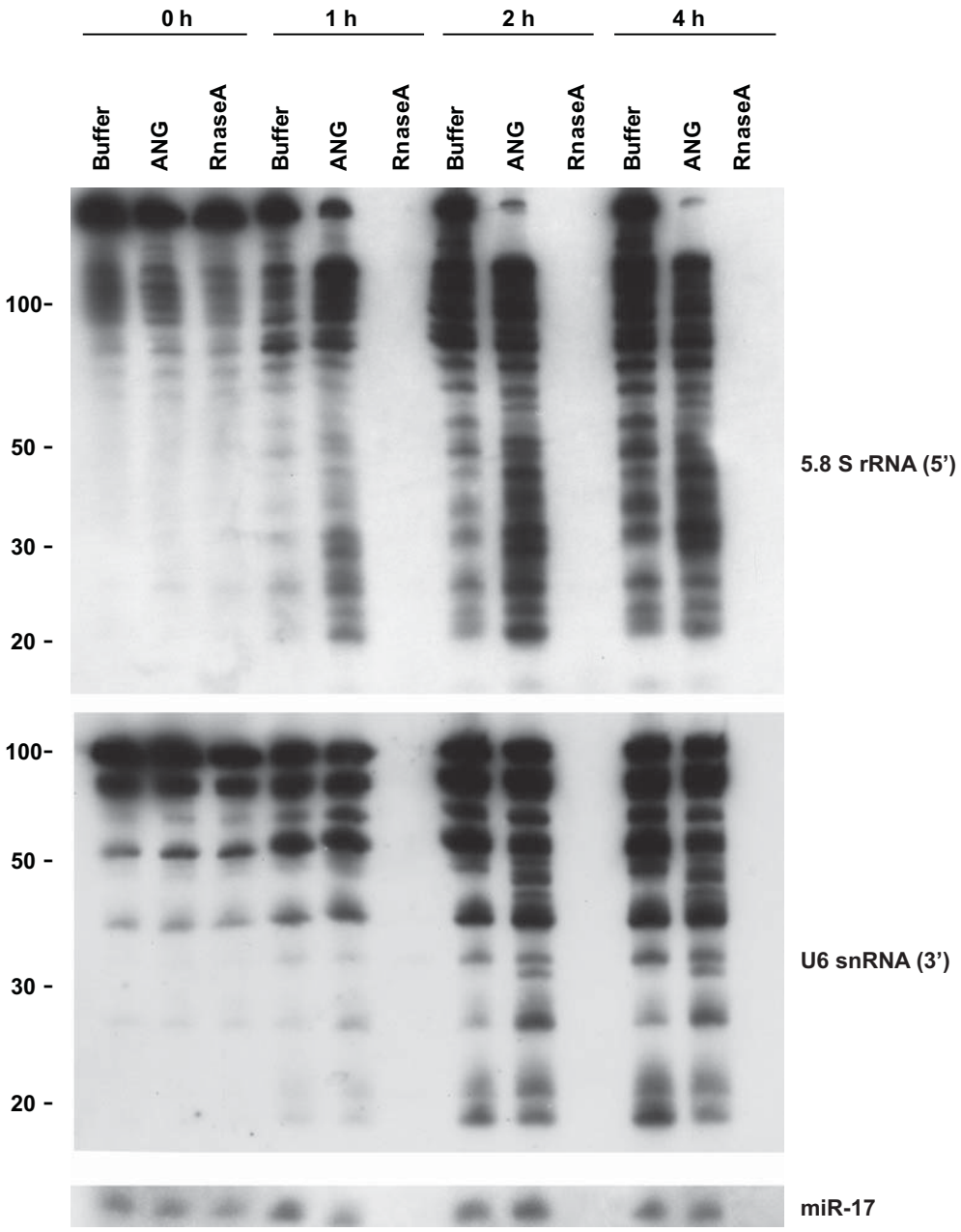

Fig S8. In vitro cleavage assay of 5.8S rRNA and U6 snRNA. Total RNA from 293 cells were treated with ANG (10 μg/ml), buffer control, or RNase A for different time periods and subjected to northern blot using probes against the 5' terminal of 5.8 S rRNA (upper) or 3' terminal of U6 snRNA (middle). The same membrane was stripped and re-probed with a miR-17 probe to ensure equal loading of RNA in all lanes.

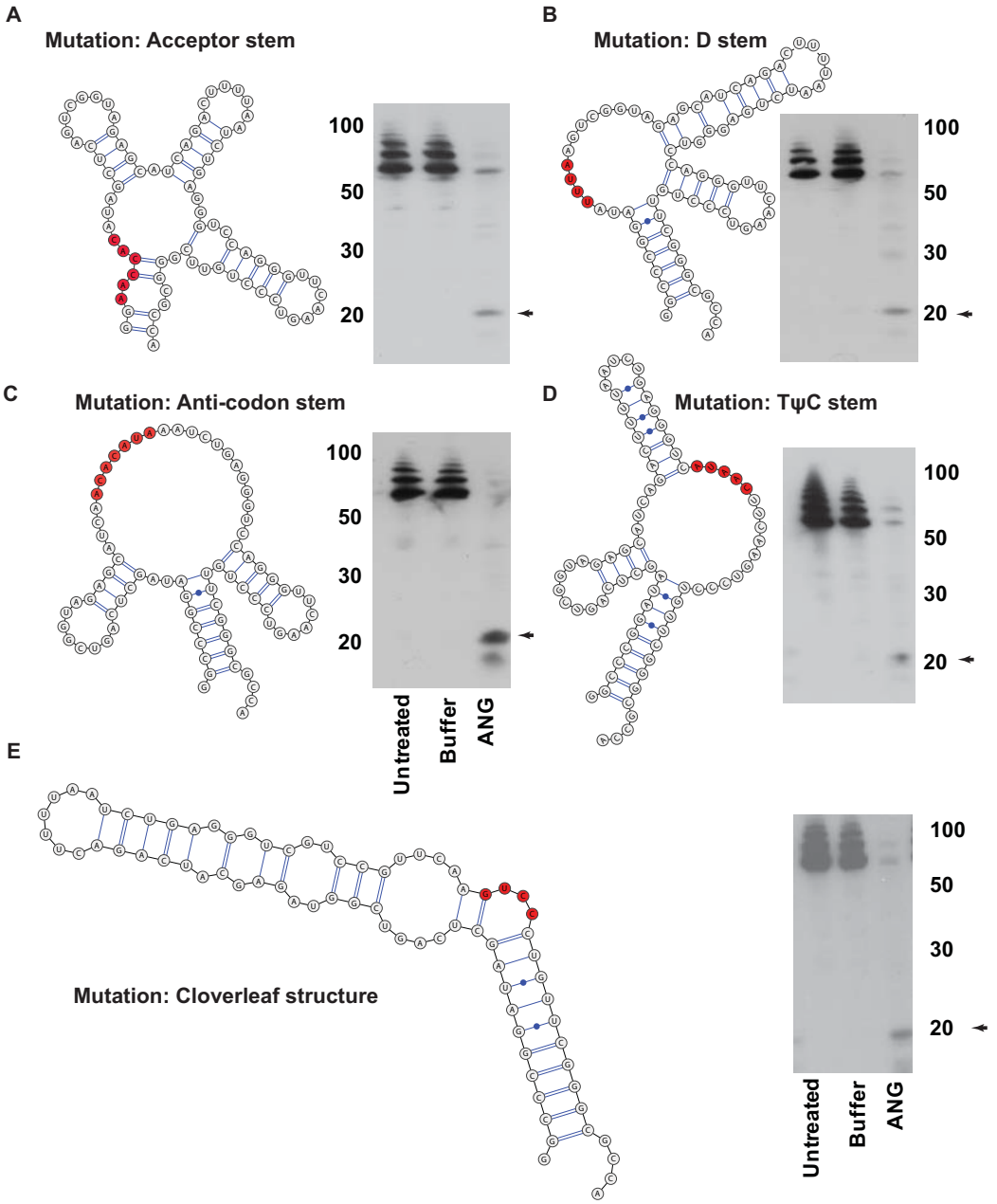

Figure S9. Effect of various mutations on ANG processing of tRFs. tRNA molecules with mutations (red) that disrupt specific tRNA sub-structures were subject to cleavage by ANG (0.5 h). Working buffer is used as a control. The disrupted structures include the acceptor stem (**A**), the D stem (**B**), the anti-codon stem (**C**) the TψC stem (**D**), and the entire clover-leaf structure (**E**). None of these mutations greatly affects tRF processing by ANG.